Journal of Optoelectronics and Advanced Materials Vol. 7, No. 5, October 2005, p. 2255 - 2266

ELLIPSOMETRY AND AFM STUDY OF POST-DEPOSITION TRANSFORMATIONS IN VACUUM-EVAPORATED As-S-Se FILMS

M. V. Sopinskyy*, P. E. Shepeliavyi, A. V. Stronski, E. F. Venger

V. Lashkaryov Institute of Semiconductor Physics, NASU, 41 Prospect Nauky, Kyiv, 03028, Ukraine

The results of multiangle ellipsometrical measurements of thermal evaporation deposited binary and pseudobinary $As_2S_xSe_{1-x}$ (x = 0,1,2,3) films are presented. Measurements were carried out for the storage time interval in the laboratory conditions from several minutes up to several years. The time dependencies of ellipsometrical parameters Ψ, Δ show the presence of the opposite Ψ and Δ evolution processes. Ellipsometrical modeling of the experimental dependencies was carried out using five models, which allowed to evaluate isotropy, uniformity, absorption of the deposited films, as well as the evolution of these characteristics with the storage time, time dependence of refractive index, and thickness. The results of this modeling are compared with the results of morphology study of film surface by AFM method. Physical analysis of the calculated parameters kinetics of the model leads to conclusion that, at the initial stage of the storage, the transformations determined by the short range scale processes are prevailing in the film. At a further stage, the prevailing processes are the ones of the middle range order and on the macroscale, which includes mass-transfer in the film and on its surface.

(Received August 24, 2005; accepted September 22, 2005)

Keywords: Ellipsometry, Post-deposition transformations, As-S-Se films

1. Introduction

The storage studies of amorphous chalcogenide films are not only of theoretical but also of practical interest. These films have numerous applications in the areas of holographic optical elements, waveguides, coatings, optical recording media, sensors, and lithography, as well as in the other areas [1-4]. Storage processes can considerably change the properties of the films thus influencing their applications.

The films' thermal deposition in vacuum on a glass substrate will result in some excess of free energy as compared with corresponding thermodynamic equilibrium state because of the structural disorder (i.e., distortions in bond angles and bond lengths) [5, 6], compositional disorder [7] (homopolar bonds are present in the film after evaporation [8-12], whose recombination is energetically profitable [13]), and non-homogeneity (i.e., pores, voids) [5-6, 8]. This stored excess free energy decreases with time due to relaxation structural changes. Unlike the studies of structural transformations in chalcogenide films stimulated by high-temperature ($T \leq T_g$) annealing or by light, the room temperature research is insufficient. Some of those results are presented in [14 - 20]. Possible influence of ambient atmosphere should be taken into account during such studies [21].

In present work, the time evolution of the ellipsometric parameters Ψ, Δ of thermally evaporated As-S-Se thin (~0.3 μm) films depending on their storage in the air at room temperature are presented and interpreted. Samples were kept in the darkness during storage. Also are presented the results of the film surface morphology study by the AFM method.

* Corresponding author: sopinsky@isp.kiev.ua

2. Experimental details.

The ~0.3 μm thick films were deposited by thermal evaporation in a chamber at a $p \sim 1\times10^{-3}$ Pa pressure using the open tantalum boat with chalcogenide glass of respective composition and onto the clean glass substrates kept at room temperature. The deposition rate (~3 nm/s) was measured continuously using the quartz microbalance technique. Deposition time was ~100 c. In ~100 c after the end of deposition the air was admitted into the vacuum chamber, the samples were removed and positioned on the measurement table of laser ellipsometer LEF-3M-1 (λ = 632.8 nm). The whole process took place in the darkness.

During the first 10 hours of storage the measurements of Ψ, Δ were carried out for four incidence angles φ_0: 67.5, 60, 52.5, 45°. Afterwards the samples were stored in dark plastic box, from which they were taken only for further measurements of Ψ, Δ angle dependencies.

In order to prevent the possible laser radiation influence the initial intensity was lowered by the absorption filter to the minimal acceptable level determined by the sensitivity of the registering system (from ~0.5 mW up < 0.01 mW). In order to decrease the measurement time the two-zone method was used, with the ~ 6 min duration. Special measurements confirmed that in these particular experimental conditions the laser radiation had no significant influence on the investigated films.

Surface morphology was studied using a scanning probe microscope Dimension-3000.

3. Results and discussion

3.1. The approach used for ellipsometric modeling.

Ellipsometers measure the complex amplitude reflection *ratio* ρ = Rp/Rs which is generally written [22, 23] in terms of two ellipsometrical angles (parameters) Ψ and Δ such that

$$\rho = Rp/Rs = \tan\Psi\exp(j\Delta), \quad (1)$$

where $\tan\Psi = |Rp/Rs|$ represents the relative attenuation of the p- and s-polarized components while $\Delta = \delta rp - \delta rs$ represents the relative phase shift.

Equation (1) is the basic ellipsometrical equation. It is the transcendental one. One of the major problems of ellipsometry is, in general, it is not possible to invert the Fresnel equations to obtain the complex refractive index parameters. Instead, the optical model has to be developed. The solution of the reverse problem is to find such values of optical constants and layer thicknesses that provide the best match between the calculated dependencies of $\Psi_{model}(\varphi_i, B)$ and $\Delta_{model}(\varphi_i, B)$ using the certain model, and the experimental dependencies of $\Psi\exp(\varphi_i)$ and $\Delta\exp(\varphi_i)$.
Here $B = (b_1, b_2, ... b_m)$ is a parametric vector which characterizes the sample under investigation. The values of parameters for the models used by us were obtained by minimizing the object function:

$$G(B) = \sum_{i=1}^{N}\left\{(\Psi_{exp}(\varphi_i) - \Psi_{model}(\varphi_i, B))^2 + (\Delta_{exp}(\varphi_i) - \Delta_{model}(\varphi_i, B))^2\right\} \quad (2)$$

Here N is the number of angles of incidence. The search of its minimum (G_{min}) was carried out using the modified Nelder-Mead method [24].

To obtain the unique model parameter values it is necessary to satisfy the $M >> L$ condition, where M is the number of the experimentally measured ellipsometric parameters, and L is the quantity of the obtained parameters of the model [22, 23]. The further complication is that the difficulty of the evaluation of the error function global minimum increases with the increase in the number of the searched parameters. The reasonable course of action in our case is to determine the character of the processes which take place in the films by using the simplest models with the

minimal number of parameters. Besides G_{min}, the important model adequacy evaluation criterion is the physical basis of the obtained solution, and also the match among the properties of thermally evaporated films obtained by other independent methods, including those obtained by other authors. Such an approach was realized in the present work.

3.2. Evolution of the Ψ, Δ experimental values with storage.

The character of changes for ellipsometrical parameters Ψ, Δ with storage is qualitatively similar for all incidence angles. Thus, Ψ, Δ measured for different films with storage time are presented for incidence angle 45° (Fig. 1a and 1b).

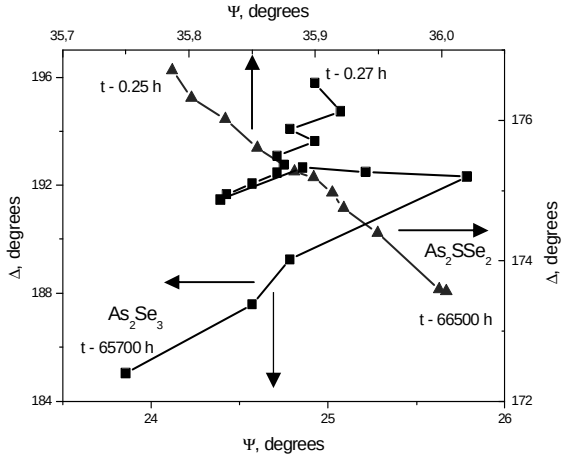

Fig. 1a. Evolution of ellipsometric parameters during storage of As_2Se_3 and As_2SSe_2 films.

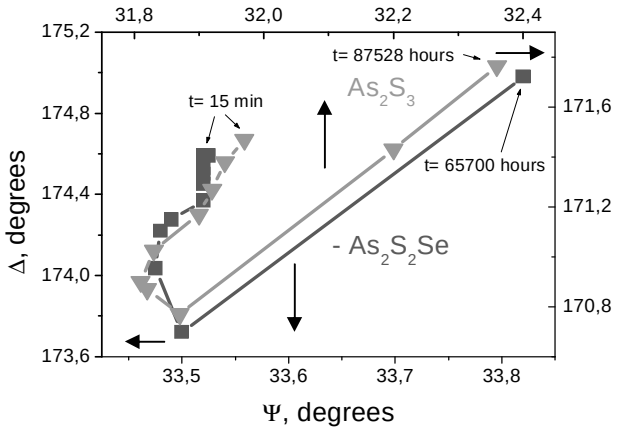

Fig.1b. Evolution of ellipsometrical parameters during storage of As_2S_3 and As_2S_2Se films.

The decrease of Δ_{45} with time is primarily observed for the As_2Se_3 film, while behavior of Ψ_{45} is more fluctuational. For the As_2SSe_2 film, the monotonous decrease of both Ψ_{45} and Δ_{45} takes place. Trajectories of Ψ_{45}, Δ_{45} are non-monotonous, and very similar for the As_2S_3 and the As_2S_2Se films. At the initial stage (approximately first day) the values of both parameters decrease. During the middle interval ~ 24-3000 hours the Δ_{45} continues to decrease, while the ψ_{45} reverses the direction of its change and increases. At the final stage (t > 3000 hours) the increase of Δ_{45} is observed. After the long storage the Δ_{45} and Ψ_{45} values are substantially greater than the ones of the

freshly-evaporated film.

This semi-qualitative analysis clearly shows that we observed at least two simultaneous or subsequent different processes taking place in sulfur-enriched films, with some prevailing first, while some other prevailing later. However, it is difficult to judge the progress of qualitatively differing processes in As_2Se_3 and As_2SSe_2 films by raw $\Psi(t)$, $\Delta(t)$ data. Also, it should be mentioned that the greater is the Se content the greater is the range of changes for Ψ and Δ.

More information about the peculiarities of the films storage behavior can be obtained by ellipsometrical modelling.

3.3 Study of temporary evolution of $As_2S_XSe_{1-X}$ films on the basis of the "single isotropic uniform absorbing layer" model.

Most often the researchers dealing with the optical constants and thickness measurements of the amorphous chalcogenide films treat them as the uniform and isotropic layers. Generally speaking, the parameter values obtained within the framework of these models represent more or less averaged effective parameters of the real films.

Time dependences for refractive index *n*, thickness *h* and absorption index *k* calculated within the framework of the uniform isotropic layer model are shown in the Fig. 2a, 2b, 2c.

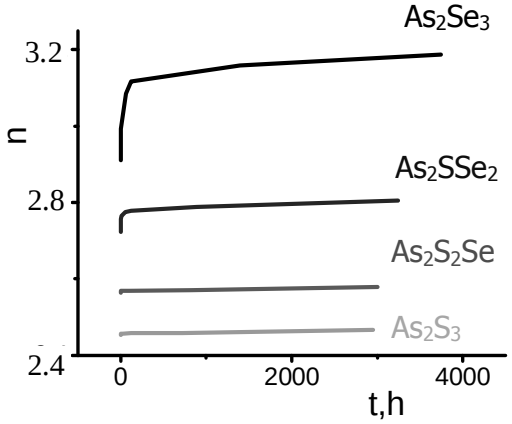

Fig. 2a. Storage time evolution of refractive index for different As-S-Se compositions.

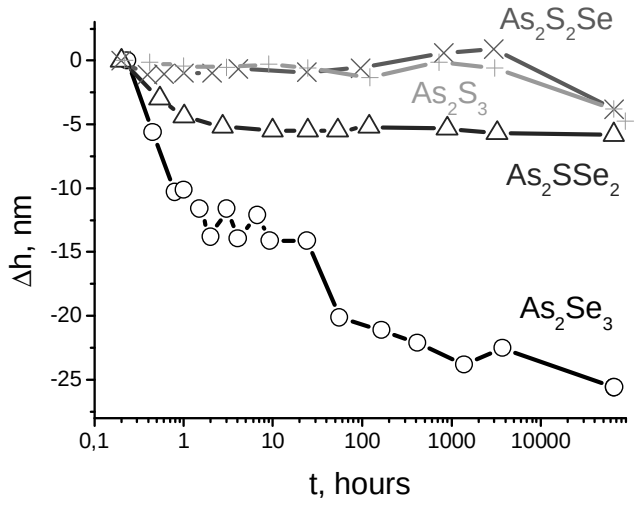

Fig. 2b. Change of the film thickness with storage time for different As-S-Se compositions.

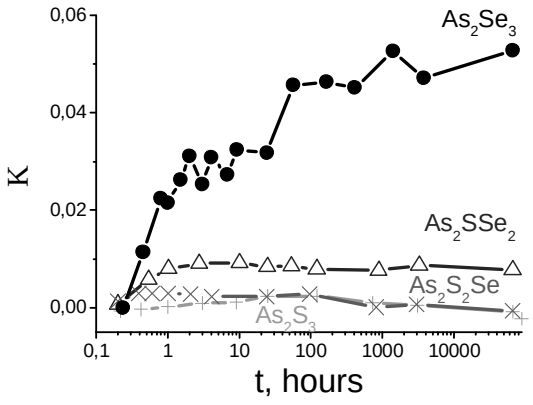

Fig. 2c. Storage time evolution of absorption index for different As-S-Se compositions.

Three regularities can be easily seen for time dependencies of refractive index:
- narrowing of range for index changes with increase of sulfur content;
- rapid change in the refractive index at the earlier stages of aging, followed by slower change at the later stages;
- the substitution of one-third of Se atoms by S atoms causes much greater difference in *n(t)* dependence than the substitution of one-third of S atoms by Se atoms.

The probe light wavelength of λ = 632.8 nm is located at the optical absorption edge of $As_2S_xSe_{3-x}$ films. The change in *n* at this wavelength can be caused by the shift of the edge, and accordingly, by the shift of dispersion curve $n(\lambda)$ [25]. In turn, the shift of optical absorption edge is caused by the change of the film microstructure, that is, in case of the amorphous films, by the change of parameters describing the short- and medium-range order. On the other hand, the change in *n* can be caused as well by the change of film macrostructure, such as its texture, and degree of macroscopic compactness [6].

The value of the film thickness changes correlates with the value of the refractive index change - the difference in the ranges of thickness change for the As_2Se_3 and As_2SSe_2 films is substantially greater than that for the As_2S_3 and As_2S_2Se films.

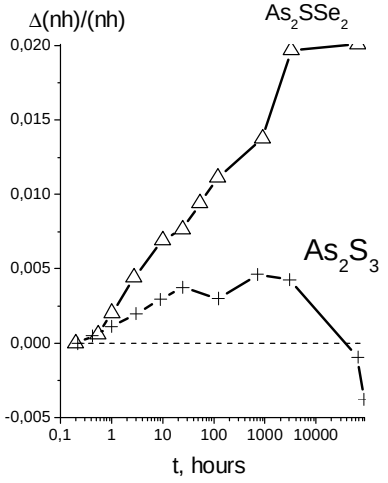

Fig. 3 Relative change of the optical thickness of the films during storage.

It is necessary to note that, according to our data, in first minutes immediately after the end

of deposition, the thickness of As_2Se_3 film decreases while the thickness of As_2S_3 film increases. This is in agreement with the results of authors [16], who established that As_2S_3 films deposited on the substrate kept at room temperature are characterized by the compression stress that relaxes towards increasing after evaporator is switched off. At the same time the As_2Se_3 films are characterized only by the stretching stress that relaxes towards increasing after evaporator is switched off.

It should also be noted that in case of Se-enriched films the main changes in the film thickness occur during the starting stage of storage whereas for S-enriched films they occur during the final stage.

Fig. 3 compares relative changes in optical thickness for Se- and S- enriched films. We can see that in the first case the films' optical thickness increases to saturation value with storage time. In the second case the initial increase of *nh* is followed by its decrease at long storage times. Such behavior of *nh* is connected with the predomination of refractive index changes for As_2Se_3 and As_2SSe_2 films, and thickness changes for As_2S_3 and As_2S_2Se films. The predomination of thickness changes for As_2S_3 and As_2S_2Se films may be caused by desorption of sulfur-rich from these films. In our opinion, the proof of such desorption is the tarnishing of the evaporated silver film when it was stored in the small closed box in close proximity from the As_2S_3 film, and the absence of the visible tarnishing after storage near the As_2Se_3 film.

For As_2Se_3 film the *k* increases from low values corresponding to the exponential tail region, and up to the values corresponding to the region of inter-band optical transitions ($\alpha \geq 10^4$ cm^{-1}). This indicates the presence of long-wave shift in the fundamental optical absorption due to the polymerization process. For the As_2Se_3 film the substitution of one selenium atom by sulfur leads to the essential decrease of *k*, while for the As_2S_3 film the substitution of 1/3 of sulfur atoms by Se does not cause essential changes in *k*. Thus, it can be seen that the difference in time behavior of all three parameters *n, h, k* for As_2Se_3 and As_2SSe_2 films is more pronounced than for As_2S_3 and As_2S_2Se films.

Using the values of *n, k, h* calculated within the framework of the single isotropic uniform absorbing layer model, we established [19] that, at the first (initial) stage of storage, the kinetic dependencies of refractive index change with reasonable accuracy can be described by the exponential dependence of $\Delta n(t) \sim exp(-t)$ type. On the second stage they can be described by the logarithmic $\Delta n(t) \sim ln(t)$ dependence. The storage time behavior of the absorption index is described by the similar dependencies only at the first stage, where the *k* increases for all films. On the second stage the slight increase in *k* is observed only for As_2Se_3 film, while for other compositions the slight decrease in *k* is observed.

The thickness changes for As_2Se_3 and As_2SSe_2 films are characterized by the exponential decay of *h*. The duration of the first stage was ~ 10 hours for $x = 0, 1$; several hundred hours for $x = 2$, and ≥ 1000 hours for $x = 3$.

During the analysis of the $\Delta n(t)$, $\Delta k(t)$, $\Delta h(t)$ kinetic dependencies and quantitative values of their parameters the presence of micro- (nano-) and macro-heterogenic structure of the initial state for the as-evaporated films should be taken into account.

The structure of evaporated $As_2S_xSe_{3-x}$ films can be represented in form of a matrix that consists of pyramidal units of $AsSe(S)_{3/2}$. This matrix also contains considerable amounts of $As_4Se(S)_4$ and $Se(S)_2$ fragments that contain As-As and Se(S)-Se(S) homopolar "wrong" bonds [7, 10-11]. (Sub)macroscopic defects (pores, hollows, flaws, etc.) are present in films as well [8]. Molecular fragments observed in as-evaporated $As_{40}S_xSe_{60-x}$ films are related to the molecular composition of vapor, which is partially frozen during condensation onto substrate. In $As_2S_xSe_{3-x}$ vapor the various $As_lS_mSe_n$, clusters are present. During condensation these molecular fragments recombine with each other to form a network with bond distribution close to a random one. Thus, in as-evaporated films the homopolar bonds as well as the other "wrong" bonds are present (dangling or non-terminating). The concentration of molecular fragments containing homopolar bonds in as-evaporated As_2S_3 and As_2Se_3 films was estimated as ~30 at% [9, 26].

The exposure or annealing of the films leads to stabilization of the local structure through redistribution of chemical bonds of the nearest environment, as well as the interaction between the As and S(Se) rich molecular fragments. Such decrease of homopolar bonds number is favored thermodynamically [13]. Data presented in the Table below serve as the substantiation of this for As-S(Se) films [13]:

Bond	As-As	S-S	Se-Se	As-S	As-Se
Bond energy, eV	2.07	2.69	2.14	2.48	2.26

From this data we obtain:

2E(As-Se) - E(As-As) - E(Se-Se) = 4.52 – 2.07 – 2.14 = 0.31 eV;
2E(As-S) - E(As-As) - E(S-S) = 4.96 – 2.07 – 2.69 = 0.20 eV;

As we have seen, polymerization process is more energetically favorable for Se-enriched film as compared to the S-enriched films. Besides, for polymerization process in S-enriched films it is necessary to break the rather strong S-S bond. By these two circumstances it is possible to explain enough slower polymerization process in $As_2S_xSe_{3-x}$ films enriched by sulfur in comparison to the films enriched by selenium.

The influence of diffusion processes is negligible at this stage due to the high concentration of As-As and S(Se)-S(Se) rich molecular fragments (see above, ~30 at.%) in fresh as-evaporated films. Those fragments are in the closest proximity to each other, such as the cube with the side length of ~ 2 atoms. Thus, the change in the number of As-As and S(Se)-S(Se) rich molecular fragments N_H and, respectively, the number of homopolar bonds in the course of annealing can be described by

$$dN_H/dt = - CN_H \quad , \tag{3}$$

where C is constant. Solution of Eq. (3) gives

$$N_H (t) = N_H (0) \exp(-Ct), \tag{4}$$

where $N_H(0)$ is the number of As-As and S(Se)-S(Se) rich molecular fragments (and number of respective homopolar bonds) at the initial stage of as-evaporated films, and t is the annealing time.

Similar considerations can also be used to describe the temporary changes of the local atom displacements without breaking and re-switching of bonds, but only including the displacements leading to the decrease of the film free volume. In this case we must replace the number of the available structural units containing homopolar bonds with the number of free places (free volume species) in the film in which the atoms displacements are possible. This leads to the decrease in the number of such places (decrease of the free volume). Such atomic displacements without switching of bonds will cause only the intermediate range order changes, which are characterized by the increase in the structural ordering of the film.

Further, with the decreasing number of As-As and S(Se)-S(Se) rich molecular fragments and increasing distances between them, the role of diffusion processes should increase. Such processes have, as a rule, the parabolic temporal dependence. However, the logarithmic law is also observed. For instance, in [27] it was established that the diffusion-controlled process of copper film chlorination follows the logarithmic law. It is also necessary to note that the logarithmic dependence $\Delta n(t)$ was observed for light exposure of As_3Se_3 film with $\lambda = 633$ nm [28].

Thus, our approach leads to the conclusion that, at the first stage of low (room) temperature annealing of the films the local character structural transformations prevail (within the region of short-range order). During the second stage the main contribution to the changes in optical constants and thickness is ascribed to structural transformations connected with the processes involving distances on the bigger scale (medium range order level and/or macrolevel).

3.4. Study of evolution of surface roughness, absorption, non-uniformity of properties with thickness, and anisotropy of As_2S_3 film based upon the comparative analysis of three-parameter models. AFM results and their correlation with ellipsometry ones.

For many practical tasks it would be sufficient to use the “single isotropic uniform absorbing layer model” (IUAL-model) when describing the As-S-Se films. Based upon this model, it is also possible to make certain conclusions regarding the physics of the transformation processes during

the films' storage.

The possible difference in the properties of the real film and the IUAL-model can be attributed to the influence of one or more factors - non-uniformity of the properties with thickness, anisotropy, and surface roughness. In order to obtain the more comprehensive information on the structural evolution of As_2S_3 film, four ellipsometrical models were used here. These models estimate absorption, isotropy, uniformity of the film, and its surface roughness. Additionally, the AFM was used to verify the conclusions based on the ellipsometric modeling surface morphology of the film.

We chose the technological scheme that minimizes the non-uniformity of the film composition with thickness. However, the presence of the smooth non-uniformity of the composition (and thus the properties) of As_2S_3 film due to peculiarities of technology and evaporation regime cannot be excluded [29].

Based upon the waveguide measurements for waveguide modes of different polarization, the presence of the anisotropy in freshly evaporated films was assumed in [20].

In [30] it was shown, that introduction of the surface layer with n=1.46 considerably improves the accuracy of the Δ and Ψ spectral dependencies for thermally evaporated As_2S_3 films. This allows assuming the presence of surface roughness, which with some degree of reliability describes the film by the introduction of the effective surface layer, the refractive index value of which is between the values for the film volume and air.

Due to the more detailed and complete description, one might hope that such a method would sufficiently improve the understanding of the transformation processes' physical nature by adding the touches that cannot be revealed by considering the simplest model. In the present work, the models with three variable parameters were utilized. This enables individual evaluation of the presence and evolution of the absorption, anisotropy, non-uniformity of the optical properties over the thickness, and presence of the surface layer (primarily due to the roughness). These models treat the As_2S_3 film as:

- isotropic uniform absorbing layer with n, k, h (IUAL - model);
- single-axis anisotropic uniform non-absorbing layer (AUNL-model) with n_o, n_e, h;
- isotropic linearly non-uniform on $\varepsilon = n^2$ non-absorbing layer (INNL-model) with n_d, n_u, h;
- two isotropic uniform non-absorbing layers (2IUNL -model) with n_1, h_1, h_2 at n_2= 1.46.

Initially, the first three models were used to monitor the changes inside the film, while the last one was used for the surface.

Fig. 4 demonstrates the time dependencies of minima of error function G_{min} for the abovementioned three parametric models. They were normalized using the minimum value for the error function for the two-parameter "single isotropic uniform non-absorbing layer" model.

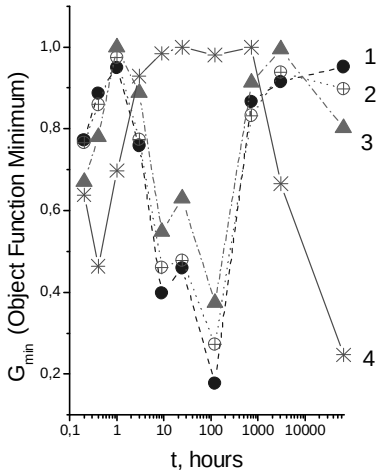

Fig. 4 1-isotropic uniform absorbing layer, b = N,K,h; 2- anisotropic uniform non-absorbing layer b = (No,Ne, h) 3- isotropic non – uniform non-absorbing layer, b=(Nb,Nu, h); 4 - two isotropic uniform non-absorbing layers, b=(N1,h1,h2, N2=1.46).

It can be seen that the time dependencies of G_{min} for the models describing the changes of different volume properties of the film have rather similar time character. They have the opposite phase compared to the G_{min} dependency for the model that describes the film surface influence. These results show that, in the given experimental situation, the multiangle ellipsometry is better for evaluation of the difference in the film volume optical properties as well as its subsurface region optical properties. It is not as good for evaluation of the properties difference of the film thickness due to the presence of absorption, anisotropy, or smooth non-uniformity of the film properties over the thickness.

One can also see that the 2IUNL -model yields the lowest G_{min} values for the initial period as well as for the long storage times, while for the middle time interval the IUAL - model yields the lowest G_{min} values. Thus, in our case it is better to analyze the kinetics of the changes of the film properties through the combination of the results for these two models.

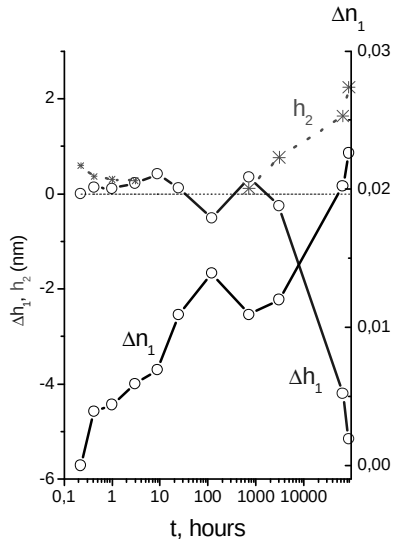

Fig. 5 Time evolution of refractive index and thickness change for As_2S_3 film and its surface layer within the frames of combined two-non-absorbing layers and single absorbing isotropic layer models.

Fig. 5 shows the changes of the refractive index and thickness in main volume of the As_2S_3 film over time. It also shows the thickness changes of its (rough) subsurface layer, obtained from the joint consideration of the results of 2IUNL and IUAL models. For each time interval, these values were calculated according to the model that yielded the lowest G_{min} values.

As can be seen, at the initial stage the thickness growth of the lower layer is approximately twice as small as compared to the thickness decrease of the upper rough layer. This leads us to conclude that only the smoothing of its surface takes place. Increase of n for As_2S_3 film without decrease of its thickness indicates that at this stage the increase of quantity and/or polarizability of bonds are taking place. These circumstances indicate that for the initial time interval the decrease of the number of broken bonds and/or replacement of the homopolar bonds by heteropolar ones take place.

For the long storage times it is quite the opposite - the thickness decrease of the lower layer is approximately two times greater than the thickness growth of the upper rough layer. Thus, here takes place not only the increase of the surface roughness of the film, but also the decrease of the total film thickness determined by its densification or partial desorption.

The results of the AFM study (Fig. 6) support the ellipsometrical results. The morphology of surface after the long storage time is characterized with the following statistics: background roughness (excluding hillocks) is Rms = 0.9 nm; overall roughness (including hillocks) is ~ 4.5 nm; hillocks mean diameter ~ 96 nm; mean distance between hillocks ~ 0.5 μm; hillocks cover ~ 4.4% of film surface. As can be seen from this statistics, the background roughness increases with storage time as compared to the freshly evaporated films (for As_2S_3 film stored several days the Rms is ~ 0.3 nm). Besides, the hillocks appear on the surface of the film.

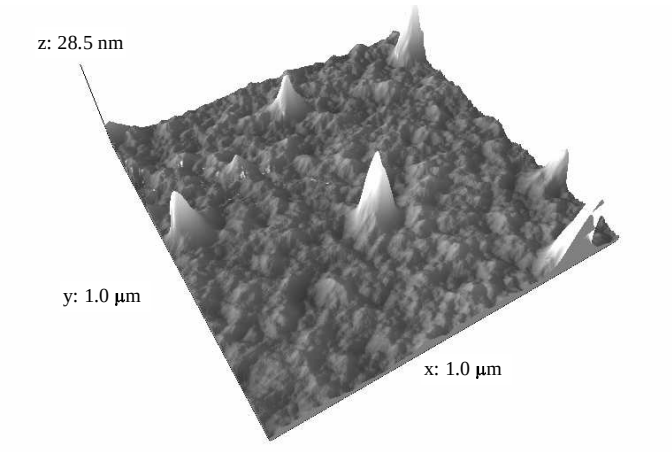

Fig. 6. AFM picture of surface morphology for As_2S_3 film stored 10 years.

The changes of the films' properties during storage can result not only from the relaxation-caused changes in structure, but also from the influence of the atmospheric oxygen. It can be assumed that the hillocks observed using the atom force microscope comprise the arsenic oxide phase. The oxygen forms strong covalent bonds both with arsenic and sulfur atoms [31], thus reducing the available As-As and S-S bonds for relaxation structural changes. Hence, the presence of oxygen, the most common element of the environment, during storage of thin amorphous chalcogenide films most probably affects the density of homopolar bonds. At the same time the oxygen affects the actual chemical composition of the surface layer, thus making this layer oxygen rich.

The formation of amorphous and crystalline As_2O_3 has been observed many times as a result of the thermal treatment and/or illumination of thin arsenic chalcogenides (see, for example, [31, 21]). Oxide fractions originated from the chalcogen atoms are high vapor pressure ones, and can (such as sulfur fractions) evaporate from film surface [32]. This way the oxygen makes surface layer of chalcogenide film also chalcogen poor.

These studies have enabled us to conclude that in $As_{40}S_{60}$ film the initial stage is accompanied by the decrease of the film roughness. Surface tends to become less irregular. At the second stage the large part of the changes in the film optical properties is caused by the reduction of film thickness accompanied by the increase of surface roughness. It is clearly caused by the structural transformations connected with the processes on a macro level scale. As a result, the sublimation of sulfur-rich components, as well as the effect of physico-chemical 'weathering' takes place during the long-time film storage. Moreover, hillock growth on the surface of the film is observed during the second stage. The hillocks are up to 20 nm in height. They occupy only the small fraction of the film surface, which may be interpreted as the slow phase transitions still in progress.

4. Conclusions

The experimental ellipsometrical investigations of the $As_2S_xSe_{3-x}$ (x = 0,1,2,3) films during storage for the time interval from 10 minutes up to 10 years have been carried out. Several ellipsometrical models were used to estimate the structure evolution of these films. Additionally, surface morphology was investigated using AFM.

In general, during storage of $As_2S_xSe_{1-x}$ (x = 0,1,2,3) films the two types of dissimilar processes are observed. Some of them are connected with the polymerization and increase of compactness, and are more pronounced in the Se-enriched films. Other processes are connected with desorption of some substitutes and influence of ambient atmosphere, and are more pronounced in the S-enriched films. It was also established that the absolute and relative changes of the refractive index

n, absorption index *k*, and thickness *h* increase with the increase of the selenium content in film composition. It was shown that the substitution of 1/3 of selenium atoms in As_2Se_3 by sulfur atoms has much greater influence on the time stability of As_2Se_3 than the substitution of 1/3 of sulfur atoms in As_2S_3 by selenium atoms on the time stability of As_2S_3.

It was established that, on the kinetic dependencies of $\Delta n(t)$, $\Delta k(t)$, and $\Delta h(t,)$ at least two stages are present, which differ in the kinetics as well as in the character of parameter changes of the films. The analysis of kinetic dependences of $\Delta n(t)$, $\Delta k(t)$, and $\Delta h(t)$ enables us to conclude that, at the initial stage of film storage, the structural transformations prevail that have local character (within the region of short-range order). They are connected with the polymerization of fragments deposited as well as the free volume reduction of the film that accompanies its structural ordering. The initial stage is accompanied by the decrease of the film roughness. Surface tends to become less irregular.

At the second stage, the main contribution to the changes in optical constants and film thickness should be ascribed to the structural transformations related to the processes involving distances on a bigger scale (medium scale order, (sub)macroscopic level scale, films' surface). Those include mass-transport processes both in the volume of film and on its surface. As a result, the sublimation of sulfur-rich components, as well as the effect of physico-chemical 'weathering' takes place during long-time film storage.

These results clearly demonstrate the importance of the kinetic studies of storage phenomena in thin amorphous chalcogenide films. Further careful kinetic investigations using other methods (X-ray, Raman spectroscopy, etc.) are necessary for deeper understanding of the processes that characterize low-temperature storage of such films.

Acknowledgements

The authors wish to acknowledge with gratitude Dr. Oksana Lytvyn (Research and Diagnostics Center of NAS UKRAINE, Kiev) assistance in the AFM experiments.

References

[1] M. Saito, Proc. SPIE **4204,** 243 (2000).
[2] I. D. Aggarwal, J. S. Sanghera, J. Optoelectron. Adv. Mater. **4**, 665 (2002).
[3] A. V. Stronski, M. Vlček, J. Optoelectron. Adv. Mater. **4**, 699 (2002).
[4] A. V. Stronski, Optoelectronics and Semiconductor Technique (in Russian) **39**, 73 (2004).
[5] J. C. Phillips, J Non-Cryst Materials **35-36**, 1157 (1980).
[6] M. Popescu, H. Bradaczek, J. Optoelectron. Adv. Mater. **1**, 5 (1999).
[7] A. Leadbetter, A. Appling, M. Daniel, J. Non-Cryst. Solids **21**, 47 (1976).
[8] D. Treasy, U. Strom, P. Klein et al., J. Non-Cryst. Solids **35-36**, (Pt.II), 1035 (1980).
[9] F. Kosek, Z. Cimpl, J. Tulka, J. Chelbny, J. Non-Cryst. Solids **90**, 401 (1987).
[10] M. Vlček, A.V. Stronski, A.Sklenar, T. Wagner, S. O. Kasap, J. Non-Cryst. Solids **266-269**, 964 (2000).
[11] A.V.Stronski Semiconductor Physics, Quantum Electronic and Optoelectronics **4**, 111 (2001).
[12] J. M. Gonzalez-Leal, Mir. Vlček, R. Prieto-Alcon, A. Stronski, T. Wagner and E. Marquez, J. Non-Cryst. Solids **326-327**, 146 (2003).
[13] K. J. Rao, R. Mohan, Solid State Communications **39**, 1065 (1980).
[14] C. A. Majid, Solid State Communications **41**, 337 (1982).
[15] B Kumar, K White, Thin Solid Films **135**, L13 (1986).
[16] M. L. Trunov, A. G. Anchugin, N. D. Savchenko, Journal of Scientific and Applied Photography (in Russian) **36**, 384 (1991).
[17] J. Teteris, I. Manica, Latvian Journal of Physics and Technical Sciences **N2**, 3 (1995).
[18] O. Nordman, N Nordman and A Ozols, Optics Communications **145**, 38 (1998).
[19] M. V. Sopinskyy, A. V. Stronski Proc. of XIIIth International Symposium on Non-oxide Glasses and New Optical Glasses, September 9-13, 2002, Pardubice, Czech Republic, University of Pardubice (2002) 201.

[20] V. I. Mikla, V. M. Kryshenik, J. Non-Cryst. Solids **330**, 33 (2003).
[21] P. Allen, B. R. Johnson, B. J. Riley, J. Optoelectron. Adv. Mater. **7**(4), 1759 (2005).
[22] R. M. A. Azzam, N. M. Bashara, (1986) Ellipsometry and Polarized Light (Amsterdam: North-Holland).
[23] T. E. Jenkins, J. Phys. D: Appl. Phys. **32**, R45 (1999).
[24] J. A. Nelder, R. Mead, Comput. Jour. **7**, 308 (1965).
[25] J. C. Phillips, The fundamental Optical Spectra of Solids, Academic Press, New York, London, (1966).
[26] N. D. Aksenov, L. L. Makarov, S. B. Mamedov, in "Non-Crystalline semiconductors-89", Uzhorod, "Patent", (1989) 192.
[27] E. S. Machlin, Y. R. Zhang, Mater. Sci. Eng. **B3**, 335 (1989).
[28] A. C. van Popta, R. G. DeCorby, C. J. Haugen, T. Robinson, J. N. McMullin, D. Tonchev, S. O. Kasap, Opt. Express **10,** 639 (2002).
[29] M. V. Sopinskyy, M. T. Kostyshin, J. Optoelectron. Adv. Mater. **3**, 411 (2001).
[30] I. Ohlidal, D. Franta, M. Frumar, J. Jedelsky, J. Omasta. J. Optoelectron. Adv. Mater. **6**, 139 (2004).
[31] L. Tichy, H. Ticha, P. Nagels and E. Sleeckx, Opt Materials **4**, 771 (1995).
[32] K. S. Harshavardhan, M. S. Hegde, Phys Rev Lett **58**, 567 (1987).